Electric Fields in Active Sites: Substrate Switching from Null to Strong Fields in Thiol- and Selenol-Subtilisins†

Deendayal Dinakarpandian,‡ Bhami C. Shenoy,‡ Donald Hilvert,§ Duncan E. McRee,|| Michele McTigue,|| and Paul R. Carey*,‡

Department of Biochemistry, Case Western Reserve University, 10900 Euclid Avenue, Cleveland, Ohio 44106, Laboratorium für Organische Chemie, Swiss Federal Institute of Technology (ETH), Universitätstrasse 16, CH-8092 Zürich, Switzerland, and The Scripps Research Institute, 10550 North Torrey Pines Road, La Jolla, California 92037

Received February 3, 1999; Revised Manuscript Received March 25, 1999

ABSTRACT: Although known to be important factors in promoting catalysis, electric field effects in enzyme active sites are difficult to characterize from an experimental standpoint. Among optical probes of electric fields, Raman spectroscopy has the advantage of being able to distinguish electronic ground-state and excited-state effects. Earlier Raman studies on acyl derivatives of cysteine proteases [Doran, J. D., and Carey, P. R. (1996) *Biochemistry 35*, 12495−502], where the acyl group has extensive π-electron conjugation, showed that electric field effects in the active site manifest themselves by polarizing the π-electrons of the acyl group. Polarization gives rise to large shifts in certain Raman bands, e.g., the C═C stretching band of the α,β-unsaturated acyl group, and a large red shift in the absorption maximum. It was postulated that a major source of polarization is the α-helix dipole that originates from the α-helix terminating at the active-site cysteine of the cysteine protease family. In contrast, using the acyl group 5-methylthiophene acryloyl (5-MTA) as an active-site Raman probe, acyl enzymes of thiol- or selenol-subtilisin exhibit no polarization even though the acylating amino acid is at the terminus of an α-helix. Quantum mechanical calculations on 5-MTA ethyl thiol and selenol ethyl esters allowed us to identify the conformational states of these molecules along with their corresponding vibrational signatures. The Raman spectra of 5-MTA thiol and selenol subtilisins both showed that the acyl group binds in a single conformation in the active site that is s-trans about the ═C−C═O single bond. Moreover, the positions of the C═C stretching bands show that the acyl group is not experiencing polarization. However, the release of steric constraints in the active site by mutagenesis, by creating the N155G form of selenol-subtilisin and the P225A form of thiol-subtilisin, results in the appearance of a second conformer in the active sites that is s-cis about the ═C−C═O bond. The Raman signature of this second conformer indicates that it is strongly polarized with a permanent dipole being set up through the acyl group's π-electron chain. Molecular modeling for 5-MTA in the active sites of selenol-subtilisin and N155G selenol-subtilisin confirms the findings from Raman spectroscopic studies and identifies the active-site features that give rise to polarization. The determinants of polarization appear to be strong electron pull at the acyl carbonyl group by a combination of hydrogen bonds and the field at the N-terminus of the α-helix and electron push from a negatively charged group placed at the opposite end of the chromophore.

The active sites of enzymes frequently bring about a reorganization of electrons in the ground state of the bound substrate as a prelude to catalysis (*1*), and in many reactions, electrostatic forces are believed to make the critical contribution to rate enhancement (*2*−*4*). In many cases, these forces lead to an increased separation of charge, namely polarization, in the functional groups involved in the reaction. For instance, in serine proteases, hydrogen bonding between the carbonyl oxygen of a bound acyl group and the enzyme's oxyanion hole groups brings about an increase in the $C^{\delta+}=O^{\delta-}$ property of the carbonyl in the ground state and eventually stabilizes the tetrahedral-like transition state with its $C-O^-$ -like bond. For a series of acyl-serine proteases, in which the acyl groups have extended π-electron conjugation, it was possible to follow the vibrational frequency of the carbonyl group in unstable intermediates by resonance Raman spectroscopy. In this series, the carbonyl frequency, which is a measure of the bond polarization, correlated with C═O bond length, strength of hydrogen bonding, and the rate of the hydrolysis reaction (*5*).

When a substrate has an extended π-electron chain, it is possible to have electron polarization that extends throughout the chain. For example, it has been shown recently that complexes of the enzyme 4-chlorobenzoate-CoA dehalogenase, with its product 4-hydroxybenzoate-CoA, exhibit very high polarization throughout the bound hydroxybenzoate group such that the ligand takes on a quinonoid-like character (*6*).

† Supported by NIH Grant GM-54072 to P.R.C.

* To whom correspondence should be addressed. E-mail: carey@biochemistry.cwru.edu. Fax (216) 368 4544.

‡ Case Western Reserve University.

§ Swiss Federal Institute of Technology (ETH).

|| The Scripps Research Institute.

10.1021/bi9902541 CCC: $18.00
Published on Web 04/30/1999

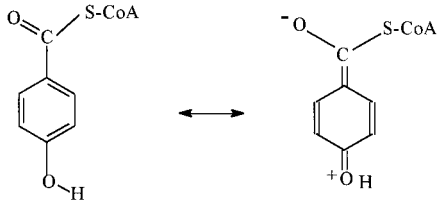

Combined crystallographic (*7*) and spectroscopic (*6*) analyses have identified the factors bringing about this radical electron rearrangement. They are strong electron pull at the benzoyl carbonyl, by hydrogen bonds combined with the electrostatic effect of the N-terminus of an α-helix, and electron push, brought about by a negatively charged aspartate side chain near the 4-hydroxy-group. Early resonance Raman (RR) studies on acyl-papains (*8*) indicated that there might be intense electron polarization forces acting in cysteine protease active sites, too. For example, the π-electrons in the chromophoric 4-(dimethylamino)-3-nitro-cinnamoyl-papain undergo such profound rearrangement upon the acyl group binding to the active site that the RR normal modes of the bound acyl group are completely reorganized compared to those of the free substrate or product. The pioneering Raman studies had to use highly colored chromophoric substrates in order to generate intense resonance Raman signals that could be detected by the low sensitivity Raman instrumentation of the time. Recently, however, due to improvements in instrumentation (*9, 10*) it has been possible to obtain Raman spectra of bound acyl-groups under normal (i.e., nonresonance) conditions. Some recent studies focused on adducts of the 5-methylthiophene acryloyl (5-MTA)[1] group with papain, cathepsin B and a number of its mutants (*11*). They confirmed that strong polarizing forces are indeed present in these active sites setting up a dipole within the acyl group.

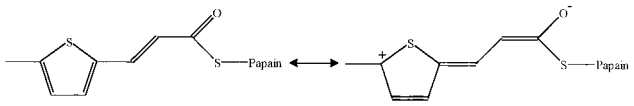

The electron reorganization is such that the acyl carbonyl is no longer a group frequency, being coupled to the ethylenic stretch and possibly other modes. Thus, C═O frequency−enzyme reactivity profiles cannot be generated within this series of 5-methylthiophene acryloyl cysteine protease intermediates. The spectroscopic signatures of a polarized acyl-group are a red-shifted λ_{max} in the absorption spectrum and a reduction in the stretching frequency for the acyl group's ethylenic linkage, $\nu_{C=C}$, in the Raman spectrum. These factors are illustrated in Table 1 for the chromophoric (5-methylthiophene) acryloyl derivatives.

For a series of acyl cysteine proteases, Doran and Carey (*11*) have shown that a linear relationship exists between the red-shift in the absorption maximum and a shift toward lower wavenumbers in the value of the acyl group's C═C stretching frequency. A shift in the absorption maximum is due to a change in the ambient electric field and is explained as follows. States possessing a dipole moment are stabilized in the presence of an electric field by an energetic amount proportional to the magnitude of the dipole moment and the strength of the electric field, due to the internal Stark effect (*12*−*14*). For groups such as the 5-MTA moiety, the larger dipole moment of the excited state compared to that of the ground state results in a red-shift of the λ_{max} in the presence of an electric field. In other words, the red-shift is seen because the excited state is stabilized to a larger degree than the ground state by the electric field. The extent of the shift is proportional to the magnitude of the electric field. While absorption spectroscopic results yield information that may be due to changes in one or both states, Raman spectroscopy focuses on the on the catalytically important ground state, as Raman peak positions are a property solely of the ground state. For acyl groups such as the 5-MTA moiety, the effect of the electric field on the ground state is seen as a decrease in the vibrational stretching frequency of the double bonds. The electric field at the active site depends not only on the charges in the structure of the protein per se but also on the reaction field set up at the dielectric boundary between protein and solvent (*13*).

Table 1: λ_{Max} and $\nu_{C=C}$ for 5-MTA- COOH, Chymotrypsin, Ethyl Thioester and Papain

compd	λ_{max} (nm)	$\nu_{C=C}$ (cm^{-1})
5-MTA acid (in CCl_4)	324	1623
acyl chymotrypsin	332	1615
5-MTA thiolester (in CCl_4)	338	1601
acyl papain	385	1576

For the acyl-cysteine proteases, much of the discussion on the causes of polarization throughout the acyl group has focused on the role of the α-helix (*11*) and the electrostatic field of its attendant dipole (*6, 12, 15*−*19*) that terminates at the active-site cysteine. It was proposed that the α-helix dipole, specifically the localized partial charges near the N-terminus, is a major factor setting up polarization in the bound thiophene acryloyl and cinnamoyl acyl groups characterized by Raman and absorption spectroscopies. Our interest in thiol and selenol derivatives of subtilisin was sparked by the fact that the sulfur or selenium atom in these semisynthetic enzymes lies at the N-terminus of an α-helix, yet little or no polarization effects have been observed in bound chromophoric acyl groups. The present work sets out to resolve this conundrum and puts forward a model to explain acyl group polarization (and lack thereof) in (5-methylthiophene) acryloyl selenol-subtilisins and thiol-subtilisins; the model itself incorporates several of the factors described above for the active site of dehalogenase.

The serine protease subtilisin (*20*) was the first enzyme to be chemically engineered to successfully generate new functionalities. The oxygen atom of the active-site acylating residue, Ser 221, has been replaced either by sulfur to generate thiol-subtilisin (*21*), or by selenium to create selenol-subtilisin (*22*). Thiolsubtilisin has been shown to have peptide ligase activity (*23*) as the acyl intermediate exhibits a marked preference for aminolysis over hydrolysis. In the case of thiol-subtilisin, the replacement of a proline residue with alanine in the α-helix that bears the acylating cysteine residue results in the enlargement of the active site due to a small displacement of the helix (*24*). This mutation has been shown to result in an enhanced preference for aminolysis. In the case of selenol-subtilisin, replacement of the putative oxyanion-hole H-bond donor, asparagine 155, by glycine also enlarges the original active site. The two forms discussed

[1] Abbreviations: 5-MTA, 5-methylthiophene acryloyl.

here, thiol-subtilisin P225A and selenol-subtilisin N155G, were selected on the basis of availability and in the expectation that an enlarged active site may result in the release of steric constraints and give rise to new conformers for the bound acyl groups. This expectation was fully realized, with the unexpected consequence that the newly observed conformers are highly polarized.

MATERIALS AND METHODS

Preparation of Acyl Enzyme. The preparation of the acylating agent used, 5-methyl-thiophene acryloyl (MTA) imidazolide, has been described previously (*25*). Acyl enzyme intermediates for each of the enzymes studied were prepared as described earlier (*26*, *27*). For example, oxidized BPN′ selenol-subtilisin was reduced under argon before the addition of the acylating agent, 5-MTA imidazolide, dissolved in DMSO. The acyl-enzyme was isolated by gel filtration on a Sephadex G-25 column, and the sample filtered through a 0.22 μM membrane before carrying out Raman spectroscopic and absorption studies. The sample used as a subtrahend was obtained by carrying out identical steps except for the addition of neat DMSO instead of substrate. The concentration of enzyme used was between 0.2 and 0.6 mM.

P225A thiol-subtilisin (*24*) was kindly provided by Dr. J. Wells, and N155G selenol-subtilisin (*28*) was kindly provided by Dr. E. Peterson.

Preparation of Model Compounds. 5-MTA acryloyl S-ethyl ester was prepared as described previously (*11*). The model compound 5-MTA Se-ethyl ester was provided by Dr. M. J. O′Connor.

Absorption Spectroscopic Studies. The determination of the λ_{max} and the rate of deacylation were carried out on a Shimadzu UV2101-PC spectrophotometer. The pK_a was calculated using the program Grafit for a single pK_a determination. To set the pH, the acyl enzyme was passed through a column containing one of various buffer systems. For both acyl enzymes the rate of deacylation was measured by following the change of absorbance at 360 nm on the spectrophotometer.

Raman Spectroscopic Studies. The Raman spectrometer used has been described previously (*9*). Raman experiments were carried out using 350 mW of the 488 nm line of an argon ion laser. Accumulation times varied from 5 to 20 min. Peak positions were calibrated using cyclohexanone as a standard and the program Spectracalc (Galactic Industries, New Hampshire). Values for well-resolved peaks are accurate to ± 1 cm^{-1}. For acyl intermediates having short half-lives, an ambient temperature of 4 ± 0.2 °C was achieved by passing a cold stream of nitrogen through a plastic jacket with an optical window that was placed around the sample cell. The stream of nitrogen was heated before reaching the sample to provide accurate control of temperature.

Molecular Modeling. For the model compounds, 5MTA thiolester and selenolester, ab initio quantum mechanical calculations with a triple-ζ potential basis set were carried out using Gaussian 94 (*29*) from Gaussian, Inc., (on either a Silicon Graphics O_2 platform or a Cray T-94 platform at the Ohio Super Computer Center) to derive the different geometries and their vibrational frequencies. Discover and Turbomole software from Biosym, Inc. (Silicon Graphics O_2 platform) were used for molecular modeling of the bound acyl group in the active site of the modified subtilisins. The consistent valence force field was modified with the addition of parameters for selenium. The coordinates of a crystal structure of selenol-subtilisin BPN′ (below) were used for the modeling. Hydrogens were built in and the structure minimized using the steepest descent algorithm (*30*) for the initial steps followed by the conjugate gradient method (*31*). The oxygen atoms bonded to the oxidized selenium atom in the crystal structure were removed and the 5-MTA moiety built in manually. Electrostatic potential derived partial charges from Gaussian 94 were used for the 5-MTA moiety. Solvent was included implicitly by the use of a linear distance dependent dielectric. The complex was locally minimized before carrying out molecular dynamics. For the latter, the protein was kept fixed except for the selenol-cysteine residue and the MTA moiety. The complex was equilibrated at 1000 K for 5 ps, and 20 sets of coordinates were saved over 2 ps. Each of the sets of coordinates was then annealed to 300 K before being minimized. The structures were screened for planarity and the presence of hydrogen bonding. Subsequently, atoms lying within 5 Å of the 5-MTA-selenol-cysteine moiety were allowed to move freely. In addition, the region lying between 5 and 10 Å of the 5-MTA-selenolcysteine moiety was partially restrained, the rest of the protein fixed, and the system minimized to convergence. For the N155G mutant of selenol-subtilisin, the additional step of replacing asparagine with glycine was carried out early in the process, with local minimization.

X-ray Crystallographic Studies of Selenolsubtilisin BPN′. Crystals of selenol-subtilisin BPN′ were grown as for subtilisin BPN′ (*32*). The data were collected using a MarResearch image plate with a Rigaku RU-200 rotating anode X-ray source. The protein crystallized in space group $P2_12_12$; $a = 85.88$, $b = 74.45$, $c = 42.43$ Å. The structure was solved by molecular replacement with XPLOR (*33*) using the coordinates of subtilisin BPN′ [PDB code 2ST1 (*32*)] as a starting model. Refinement was done using XPLOR, and the final *R*-factor was 0.202, and the resolution 8.0−2.4 Å. RMS deviations from ideality were 0.06 Å for bonds and 2.9° for angles. The coordinates have been deposited in the Protein Data Bank as entry 1UBN.

RESULTS AND DISCUSSION

Defining Conformational Markers in the Model Compounds. Analysis of the model compounds 5-MTA thiol and selenol ethyl esters provides us with a basis for interpreting the spectral data for the acyl enzymes. The ethyl group essentially substitutes for the enzyme in such calculations and provides a good starting point for interpreting the results in the active site. There are a number of advantages in choosing a conjugated compound such as the one used in this study. First, the acyl groups are strong Raman scatterers and the detection limit for Raman signals is sufficiently low to allow the collection of data at submillimolar levels. Second, definitive information about conformation may be obtained as the double bonds prevent free rotation and well-defined minima are present. Ab initio Hartree−Fock self-consistent field calculations were carried out to obtain the optimized geometries of 5-MTA thiolester and 5-MTA selenol-ester. There are two single bonds that are flanked by double bonds (Figure 1). The dihedral angle about each

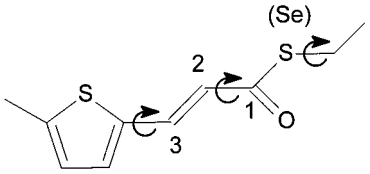

FIGURE 1: Representation of the bonds in the 5-MTA group about which rotational isomerism is possible. The isomer shown here is Cta (s-cis). Convention used for naming specific isomers is described in Results.

Table 2: HF/6-31G** SCF Energies, Dipole Moments and Boltzmann Population Distribution in Vacuo of the Rotamers of 5-Methyl Thiophene Acryloyl (5-MTA) Thiolester

rotamer	SCF energy (Δkcal/mol)	population (% at 300 K)	dipole moment (D)
Ctg	−5.151 86	88	2.6814
Cta	−3.808 99	4.6	2.6097
Ccg	−3.394 83	4.6	2.7569
Ttg	−2.943 02	2.2	3.5333
Cca	−2.127 26	0.3	2.7834
Tta	−1.625 25	0.1	3.5769
Tcg	−1.261 30	0.1	2.7706
Tca	0	0	2.8418

of the former bonds can be close to either 0 or 180°, giving rise to a total of four possible isomers. In addition, for the S−C_2H_5 and Se−C_2H_5 bonds, the methyl group can either be in the plane of the molecule or roughly orthogonal. A three-letter code has been used to denote the geometry of each isomer (Figure 1). The letters C, T, A, and G stand for cis, trans, anti and gauche, respectively. The first letter in each name refers to the orientation about the C1−C2 bond, the second describes the orientation around the C3−C4 bond, and the last represents the orientation about the C1−S bond. The term s-cis is used to describe the orientation that results in double bonds lying on the same side of an intervening single bond, e.g., C1−C2. On the basis of this nomenclature, the isomer shown in Figure 1 is the Cta isomer. Table 2 summarizes the energy of various conformers of 5-MTA thiol ethyl ester in vacuo. The difference in energy between any two conformers ranges from about 0.4 to 5 kcal/mol. The dipole moments show significant differences ranging from 2.6 to 3.5 D. The larger size of selenium required the use of the 6-311G basis set in order to keep the calculations for 5-MTA selenol ethyl ester within tractable bounds, thus a direct comparison with the thiolester results is not possible. However, the corresponding values for 5-MTA selenol-ester are qualitatively similar to those for the thiolester, e.g., the energy difference for the Ctg and Ttg conformers of the selenolester was found to be −1.63 kcal/mol compared to −2.2 kcal/mol for the sulfur analogue (Table 2).

The calculations show that the isomers that are s-cis about the C1−C2 bond are lower in energy than the counterparts that are s-trans. The Boltzmann estimate of equilibrium populations suggests that multiple conformers are likely to be present at room temperature. However, the relative abundance is likely to be strongly influenced by the dielectric constant of the solvent, as the dipole moments are different for each rotamer. Species with higher dipole moments are likely to be better represented in polar solvents. Frequency calculations of the rotamers at the Hartree−Fock level (D. D. and P. R. C., unpublished work) show that the C1−C2 bond has a fairly intense stretching mode that is sensitive to

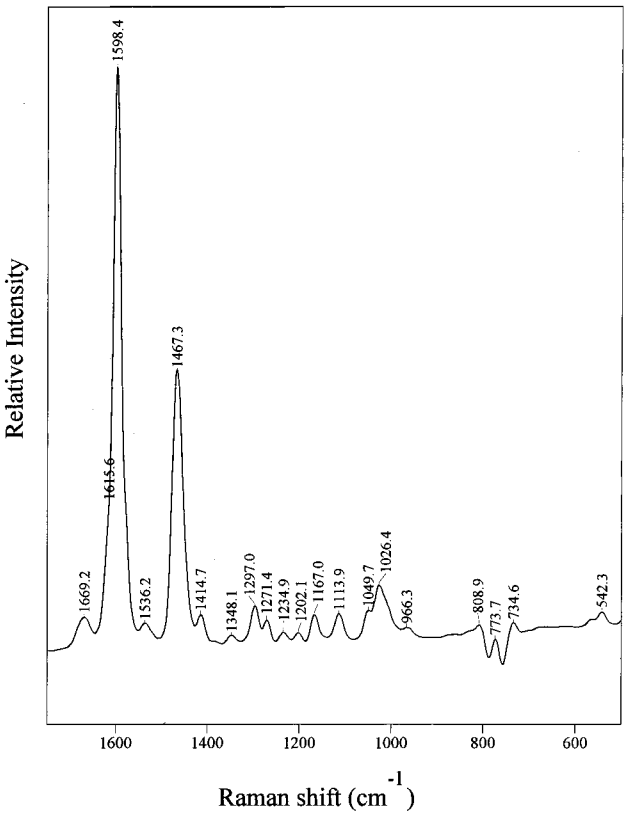

FIGURE 2: Raman difference spectrum of 5-MTA selenolester in CCl_4. Experimental conditions: 488 nm laser, 350 mW, 2 min accumulation time. The spectrum of CCl_4 has been subtracted.

rotational geometry about the bond. Hence, this mode can be used as a marker to distinguish between conformers that are cis or trans about this bond. Similar findings have been reported in earlier studies and calculations on related thiolester compounds (*26*, *34*−*36*). However, frequency differences in the case of isomerism about the other two single bonds are not as clearly discernible.

The experimental Raman data for 5-MTA thiolester have been published previously (*36*). As predicted by the calculations, Raman peaks corresponding to both s-cis and s-trans forms of the C1−C2 stretching vibrational mode are present. The Raman spectrum of 5-MTA selenol ethyl ester in CCl_4 is shown in Figure 2. In general, the spectral features are quite similar to that of the corresponding thiolester. There is clear evidence of multiple conformers as markers for both s-cis and s-trans conformers about the C1−C2 bond are seen. The marker band for the s-trans isomer occurs at 1114 cm^{-1}, against 1130 cm^{-1} in the case of the thiolester. The C1−C2 stretching frequency for the s-cis isomer is seen at 1026 cm^{-1}, close to the value of 1025 cm^{-1} in the case of the thiolester. The carbonyl stretching mode is seen at 1669 cm^{-1}, which is higher in frequency by about 16 cm^{-1} when compared to the value of 1653 cm^{-1} for the thiolester. This is probably due to partial decoupling between the carbonyl and double bond stretches because of the higher atomic weight of selenium compared to sulfur and poorer π-orbital overlap for selenium. The strong peak at 1467 cm^{-1} and the weaker peaks at 1536 and 1167 cm^{-1} are assigned to modes involving the thiophene ring. The strong feature seen at 1598 cm^{-1} is a double bond stretching mode with a weak shoulder at around 1615 cm^{-1}.

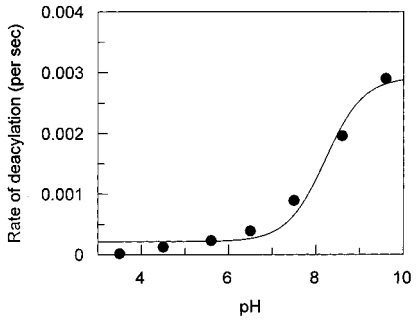

FIGURE 3: Rate of deacylation of acyl selenolsubtilisn BPN′ as a fuction of pH. Estimated pK_a = 8.2. The rate constants were measured as described in the Materials and Methods.

In the case of acyl papain, multiple conformers are seen in the experimental Raman spectrum as judged by the presence of multiple C1−C2 modes in the 1000−1150 cm^{-1} region (*11*). The position of $\nu_{C=C}$ near 1575 cm^{-1} and the red-shift in λ_{max} to near 380 nm provide clear evidence for strong polarization. Multiple conformers are also seen in acyl derivatives of the enzyme Hepatitis A viral 3C proteinase (*36*). In this case, in addition to modes involving C═C and C1−C2 stretches, evidence of heterogeneity is seen in the form of doublets in the 550 cm^{-1} region which have been assigned to vibrational modes involving the thioester linkage. As both experimental data and ab initio calculations favor the coexistence of more than one conformer for the model compound, it is foreseeable that the acyl group might adopt multiple conformations in the active sites of thiol- and selenol-subtilisin, also.

Deacylation Kinetics of the Acyl Intermediate. The observed rate of deacylation ranges from 0.000 02 to 0.0029 s^{-1} for acyl selenol-subtilisin and from 0.000 15 to 0.0011 s^{-1} for thiol-subtilisin. These values are similar to those observed for the papain family of cysteine proteases—0.000 07 to 0.015 s^{-1} at high pH (*11*). The acyl intermediate deacylates enzymatically with a single exponential. The dependence of the rate of deacylation on the pH for acyl selenolsubtilisin is shown in Figure 3. The rate shows a sigmoidal increase with a rise in pH and a pK_a value of around 8.2. The rate of catalysis is several orders of magnitude below that seen in the case of native subtilisins or papain acting on physiological substrates, but it is comparable to that reported for the rate of deacylation of *S*-cinnamoylthiol-subtilisin and Se-cinnnamoylselenol-subtilisin (*22*). The k_{lim} values in the latter case were reported to be 0.0014 s^{-1} and 0.000 71 s^{-1}, respectively. The authors reported a pK_a value of 6.8 for Se-cinnnamoyl selenol-subtilisin, which is lower than the value of 8.2 observed for 5MTA. The differences in the pK_a values can be accounted for by the different acyl groups used, by the fact that subtilisin Carlsberg was used in the early study and BPN′ in the present work, and by the likelihood that the value for 5-MTA-selenol-subtilisin is subject to some error because of the continued increase in the rate of hydrolysis at high pH. Some kinetic data for the mutants used in the study are shown in Table 3. The rate of deacylation for P225A thiol-subtilisin lies in the same range as that for thiol-subtilisin. The result obtained for the N155G seleno-subtilisin mutant is interesting in that the rate is about the same as seleno-subtilisin at pH 9.6 and even higher at pH 6.5. This is an unexpected finding because the mutation removes a potential hydrogen-bonding donor to the carbonyl oxygen of the bound acyl group in the active site. An acyl enzyme conformation derived from computer modeling described later offers an explanation for this anomalous finding.

Table 3: Rates of Deacylation and Absorption Maxima of Acyl Derivatives of BPN′ Thiol- and Selenol-Subtilisins

acyl enzyme	pH	half-life (min)	deacylation rate constant (s^{-1})	λ_{max} (nm)
thiolsubtilisin	9.6	10.2	0.0011	350
	6.5	49.2	0.000 23	355
	3.6	78.1	0.000 15	358
P225A thiolsubtilisin (subtiligase)	9.6	2.8	0.0041	361
	6.5	15.8	0.000 73	368
selenolsubtilisin	9.6	3.98	0.0029	355
	6.5	29.6	0.000 39	361
N155G selenolsubtilisin	9.6	5.2	0.0022	361
	6.5	14.66	0.000 79	367

Single Nonpolarized Conformer in the Active Site of Thiolsubtilisin and Selenolsubtilisin. The Raman spectra of 5-MTA-selenol-subtilisin BPN′ with ^{13}C labeling at positions C1 and, separately, C2 have been published earlier by O′Connor et al. (*26*). The replacement of ^{12}C with ^{13}C at the C2 position decreases the double bond stretching frequency and shifts its Raman peak away from that of the carbonyl group stretching frequency. This allows better visualization of the Raman peak corresponding to the carbonyl group stretching frequency which is otherwise seen as a weak shoulder on the strong peak of the double bond stretching frequency. The Raman spectra for acyl thiol-subtilisin and acyl selenol-subtilisin are shown in Figures 4 and 5. The data for the latter in Figure 5 are for a derivative where the C2 carbon has been labeled with ^{13}C. The double bond stretching mode is fairly intense and is seen in the unlabeled derivatives at 1606 cm^{-1} for thiol-subtilisin in Figure 4a and at 1603 cm^{-1} for selenol-subtilisin (*26*). There are multiple points of high interest here. First, the relatively high frequency of this mode is essentially the same as seen for the respective model ethyl ester compound (1602 cm^{-1} for the thiolester and 1598 cm^{-1} for the selenolester) in carbon tetrachloride. The slightly lower frequency compared to the ester compounds is probably due to the fact that the true reference state for shifts in the modes of the acyl enzyme is 5-MTA cysteine/selenolcysteine in carbon tetrachloride and not 5-MTA acryloyl S (or Se)- ethyl ester. The latter, however, serve as the best alternative. Second, no conformational heterogeneity of acyl selenosubtilisin is evident in Figure 5a. The ethylenic stretch is seen as a sharp intense feature at 1584 cm^{-1}. Only a single band corresponding to the C−C stretching mode for the s-trans isomer is seen at 1110 cm^{-1}. This finding is remarkable because the s-trans conformer is predicted to have a higher energy than the s-cis conformer, based on the ab initio calculations on the model compound, and yet the enzyme clearly shows a preference for the former.

The lack of heterogeneity is in marked contrast to the situation in the case of papain, where at least two isomers are seen, with C1−C2 markers in both the 1100 and 1000 cm^{-1} regions. Further, in papain, the peak position of the double bond stretching frequency is downshifted by 25 cm^{-1} from the reference value in CCl_4. The lack of polarization

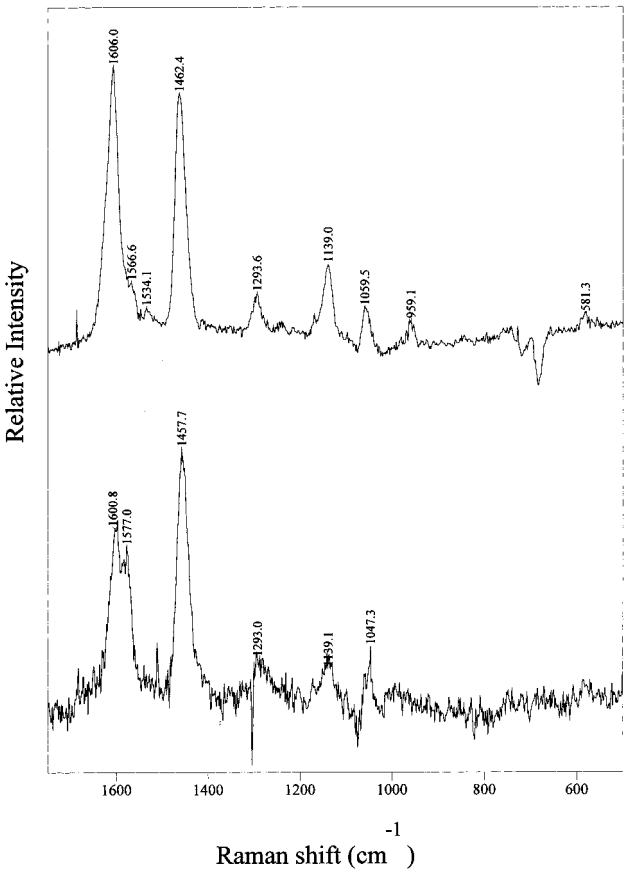

FIGURE 4: Raman difference spectra of 5-MTA thiol-subtilisin. (a) Acyl derivative of native thiol-subtilisin. (b) Acyl derivative of P225A thiol-subtilisin. Concentration of acyl derivative ~0.2 mM. Experimental conditions: 488 nm laser, 350 mW, 20 min accumulation time. Spectrum of the enzyme alone in buffer has been subtracted.

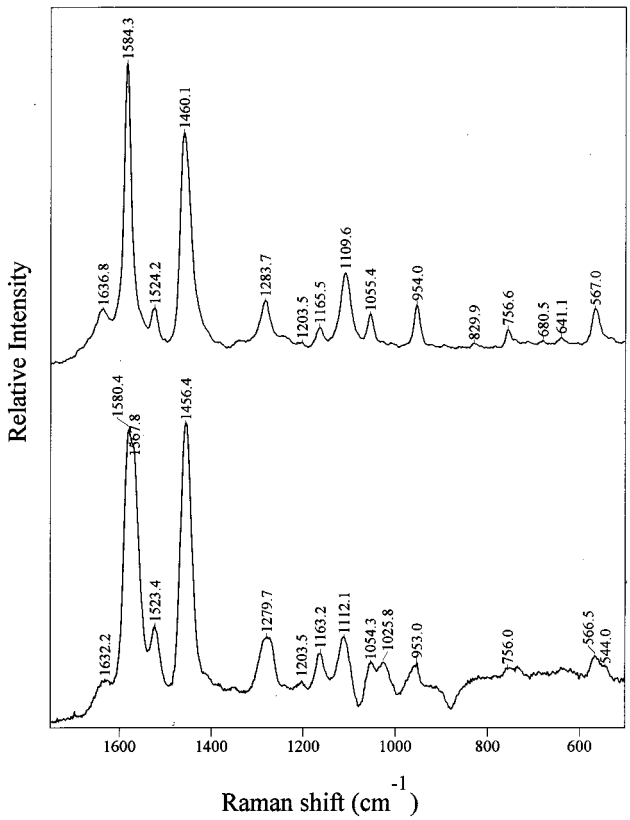

FIGURE 5: Raman difference spectra of 5-MTA selenol-subtilisin with ^{13}C labeling at C2, (a) Acyl derivative of native selenol-subtilisin. (b) Acyl derivative of N155G selenol-subtilisin. Concentration of acyl derivative 0.5 mM. Experimental conditions: 488 nm laser, 350 mW, 20 min accumulation time. Spectrum of the respective enzyme alone in buffer has been subtracted.

attested to by the near identities of $\nu_{C=C}$ for the acyl enzymes and the selenol and thiol esters corroborates the absorption spectroscopic results. The λ_{max} values for acyl thiol-subtilisin (350−358 nm) and acyl selenol-subtilisin (355−361 nm) listed in Table 3 are considerably lower than the value of 380 nm seen in the case of papain and, therefore, point to the lack of polarization of the 5-MTA group. The above findings imply one of two possibilities. There may be no electric field in the subtilisin active site that is capable of inducing polarization across the whole molecule. Alternatively, the chromophore might be locked in a conformer that is orthogonal to the electric field and thus shows no evidence of polarization. The fact that only one conformer is seen, despite the small energy differences between rotamers predicted by the ab initio calculations, lends support to the latter hypothesis. For selenol-subtilisin, the carbonyl stretch shows a downward shift from 1669 cm^{-1} (Figure 2) to about 1643 cm^{-1} (*26*). As this shift is localized to that of the carbonyl stretching frequency, it is highly suggestive of a hydrogen bonded conformation for the carbonyl group in the enzyme active site. The downshift of 26 cm^{-1} is greater than the 15 cm^{-1} estimated in an earlier publication (*26*) based on the position of $\nu_{C=O}$ for 5-MTA ethyl *thiol* ester in CCl_4. Thus, our initial conclusion that the acyl carbonyl forms only a weak hydrogen bond to the active site has to be modified to say that the C═O forms a weak-to-medium strength hydrogen bond.

Multiple Conformers and Polarization in the Active Sites of N155G Selenolsubtilisin and P225A Thiolsubtilisin. On the basis of the premise that the release of steric constraints might allow multiple conformers to be present in the active site, the mutants N155G selenol-subtilisin and P225A thiol-subtilisin were chosen for study. The N155G mutant is an oxyanion hole mutant. Apart from lowered reactivity due to loss of a potential hydrogen bond donor, an expected effect is an enlargement of space in the active site due to the absence of the side-chain amide. P225A thiol-subtilisin brings about an enlargement of the active site in a different manner (*24*). The substitution of proline with alanine leads to a removal of a kink in the helix that bears the cysteine residue that is equivalent to Ser 221. As a result, the segment of the α-helix supporting residue 221 is translated away for the active site by about 0.3 Å leading to an enlargement of the active site. The absorption data for the two mutants (Table 3) are interesting in that the λ_{max} is red-shifted in both cases. For P225A thiol-subtilisin, a shift of 11−13 nm is observed, depending on the pH, and for N155G selenol-subtilisin, a shift of 6 nm is seen. Raman spectra for the two active-site enlarging mutants used in this study are shown in Figures 4b and 5b.

The results for thiol-subtilisin are discussed first. The data in Figure 4b were obtained at concentrations close to the limits of detection but the strongest peaks, seen clearly above the noise, are the ones relevant to this discussion. The single peak corresponding to the double bond stretch for acyl thiol-subtilisin seen in Figure 4a is now seen as a doublet. The

peak seen in Figure 4a at 1606 cm^{-1} is replaced in Figure 4b by two peaks at 1601 and 1577 cm^{-1}. The s-trans isomer is now seen at 1601 cm^{-1} as a peak of lesser intensity (the ring mode at 1458 cm^{-1} serves as an internal standard for intensity). For α,β-unsaturated carbonyl compounds, the double bond stretching frequency for the s-cis isomer is predicted to have a lower vibrational frequency than the s-trans isomer (*37*, *38*). The new peak at 1577 cm^{-1} is assigned to the double bond stretching frequency for the s-cis isomer. The difference of 24 cm^{-1} between the values of the ethylenic stretching frequencies for the two conformers in P225A thiol-subtilisin is more than the expected difference between s-cis and s-trans conformers (unpublished results from calculations). The presence of two features in the C═C stretching region demonstrates that at least two isomers are present in the active site of P225A thiol-subtilisin. Moreover, the large 24 cm^{-1} downshift shows that the s-cis acyl group is under the influence of a stronger electric field than the s-trans conformer. The absence of the C1−C2 marker for the s-cis conformer is probably because the signal is obscured by the high noise level in this spectrum. Qualitatively very similar findings are seen in the case of selenol-subtilisin. In contrast to Figure 5a, the double bond mode is seen as a broad feature of lesser intensity in Figure 5b. Further, a shoulder is seen at around 1568 cm^{-1}. The single bond stretch corresponding to the s-trans conformer at 1110 cm^{-1} is reduced in intensity and shifted upward by about 2 cm^{-1}. There is the appearance of a new single bond stretching mode corresponding to the s-cis conformer at 1026 cm^{-1}. The band at 1284 cm^{-1} is replaced by a broad feature centered at 1280 cm^{-1}. In addition, the Raman peak at 567 cm^{-1} now shows a shoulder on the low wavenumber side, similar to the doublet seen in case of the acyl HAV-3C intermediate (*36*).

In essence, the release of constraints in the active site by either replacing a hydrogen bond donor residue with a smaller non-hydrogen bond donor residue or by moving the helix has allowed the generation of a new conformer. Further, the observed shifts in vibrational frequency suggest polarization of the ground state, in line with the predictions from the λ_{max} measurement. As polarization is a strongly vectorial phenomenon, the extent of the effect is dependent not only on the strength of the electric field but also on the precise alignment of polarizable bonds along the lines of force. In effect, small changes in geometry of either the active site or the bound acyl group can result in major changes in the amount of polarization observed.

Identifying the Determinants of Polarization by Molecular Modeling. Molecular modeling was undertaken in an effort to determine the structural determinants in the active site responsible for the spectroscopic findings described above. Attempts to model interactions for the P225A mutant of thiol-subtilisin were made by replacing proline with alanine. However, we conclude that the changes produced cannot be modeled accurately due to the relatively coarse nature of the force field used, thus we concentrated on modeling 5-MTA in the active site of selenol-subtilisin.

Modeling small molecules such as the 5-methyl thiophene acryloyl group used in the present study in the active site of a protein often locates more than a single minimum. This is a consequence of the relatively large active-site volume accessible to the substrate coupled with the fact that the difference in energy between two conformations is often small enough to be on the order of the intrinsic error within the force field. Thus, rather than using the values of the computed energies, the proposed structures for acyl selenol-subtilisin and acyl N155G selenol-subtilisin (Figures 6 and 7) were chosen on the basis of ab initio calculations and results from Raman spectroscopy. For instance, the 20 frames obtained for acyl selenol-subtilisin, though largely redundant, resulted in three unique structures. Only one of the three was retained as it was both hydrogen bonded (evidenced by the Raman data) and close to planarity (predicted by the ab initio calculations).

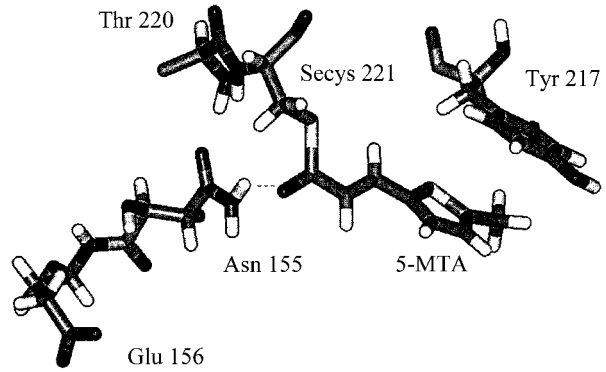

FIGURE 6: Stick representation of the molecular mechanics model for the orientation of the acyl group in the active site of selenol-subtilisin. Enzyme atoms within a radius of about 5 Å of the 5-MTA moiety alone are shown. The carbonyl oxygen is hydrogen bonded to the side chain of Asn 155. Details of the method used to obtain the model are described in the Materials and Methods.

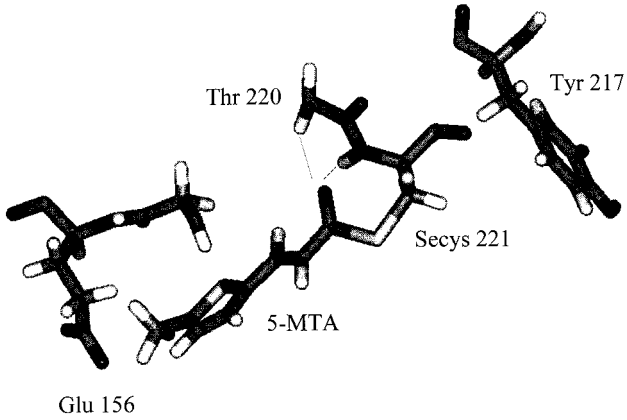

FIGURE 7: Stick representation of the molecular mechanics model for the orientation of the acyl group in the active site of the N155G mutant of selenol-subtilisin. Enzyme atoms within a radius of about 5 Å of the 5-MTA moiety alone are shown. Compared to Figure 6, the carbonyl oxygen of the acyl group is now hydrogen bonded to the backbone amides of Secys 221 and Thr 220, with the thiophene ring lying close to the side chain of Glu 156.

The final structure proposed for acyl selenol-subtilisin is shown in Figure 6. The residues believed to be responsible for the specific nature of the interaction between the 5-MTA moiety and the active site of the enzyme are shown. Atoms of the residues Ser 125, Asn 218, Gly 219, and Met 222 that lie within a radius of 5 Å of the MTA moiety have been removed for a better view of the latter. For acyl selenol-subtilisin, the carbonyl oxygen of the 5-MTA moiety is hydrogen bonded (3.0 Å) to the side-chain amide of Asn 155. The thiophene ring stacks next to the ring of Tyr 217. The conformation is s-trans about the C1−C2 bond with a

dihedral angle of 168°. On the basis of the nomenclature proposed earlier, the isomer shown is Tca. In other words, all the atoms of the MTA moiety and the carbons of the selenol-cysteine residue are more or less in the same plane. The stacking energy from interaction with the tyrosine ring is proposed as the source of stabilization of the s-trans conformer vis-à-vis the s-cis conformer. The results of modeling for the N155G mutant shown in Figure 7 help to explain why polarization is seen in this case. Some atoms have been removed for better visualization of the specific interactions in the model. There is a net translation of the acyl group in response to the new space created by the replacement of Asn 155 with a glycine residue. Confirming the findings from the Raman spectroscopic data, a new conformer of the acyl group, oriented differently from that seen for the wild type, is seen in the active site of the N155G mutant. This corresponds to the Ccg isomer. The $C_\alpha-C_\beta$ bond of the selenol-cysteine is now orthogonal to the plane of the 5-MTA moiety. The loss of hydrogen bonding to asparagine 155 is well compensated by hydrogen bonding to the backbone amides of selenol-cysteine 221 and threonine 220. Although these hydrogen bonds are not perfectly linear, the distances (2.9 and 3.0 Å) indicate that the acyl C═O lies within hydrogen-bonding distance to the backbone amide NHs. The space created by the absence of the amide group of asparagine 155 allows the group to adopt a s-cis conformation about the C−C(═O) single bond, resulting in the close proximity of the thiophene ring to the side chain of glutamate 156. As this arrangement brings the thiophene ring within 4 Å of the carboxylate group of glutamate 156, it sets up the molecular axis of conjugation in a favorable position to sense the local electric field produced by hydrogen bonds at one end and a carboxylate group at the other. Since the acylating residue lies at the amino end of an α-helix, the potential due to the helix dipole is likely to make an additional contribution to polarization extending across the π electron system. Although Braxton and Wells (*39*) have proposed that the side chain of Thr 220 forms part of the oxyanion hole WT subtilisin, no evidence was found in our calculations for an interaction between the acyl C═O moiety and the −OH group of Thr 220's side chain. However, our identification of Glu 156 as a residue that can interact with the acyl group in the N155G form is entirely consistent with the mutagenesis work of Wells et al. (*40*) that demonstrated a key electrostatic role for Glu 156 in subtilisin kinetics.

In general, the results of modeling are consonant with the experimental findings that the N155G mutant provides greater conformational flexibility for the bound acyl group. For the acyl enzyme of the mutant form the trajectory shows the acyl group "bouncing" around the active site, whereas for the wild-type intermediate it is limited to a much narrower region of conformational space.

The deacylation rate constants obtained from absorption spectroscopy seem curious in that N155G selenol-subtilisin does not show a markedly different rate from that of WT selenol-subtilisin. However, the results from molecular modeling offer an explanation in that hydrogen bonding by the backbone amides of Thr 220 and Se-Cys 221 compensates to a sufficient degree for the loss of the asparagine residue. It is interesting to note that these findings are consonant with those for cinnamoylselenol-subtilisin where the N155G variant deacylates approximately 1.5 times faster than the WT analogue (Warren and Hilvert, unpublished work). Returning to the present work, it is a moot point whether the proximity of the side chain of Glu 156 to the thiophene ring contributes to binding or also to catalysis. It is interesting to note that papain has an acid residue, Asp 158 at about the same distance from the acylating residue Cys 25 as Glu 156 is from Secys 221 in the present case. It can be hypothesized that both s-cis and s-trans forms of the 5-MTA moiety lie close to Asp 158 in the active site of papain and this contributes strongly to the polarization seen in the case of papain (*11*).

The model derived here for the polarized acyl group in the active site of N155G selenol-subtilisin is similar to the crystal structure of an enzyme product complex, namely, dehalogenase bound to *p*-hydroxy-benzoyl CoA (*6*, *7*). In the latter, very strong polarization is observed in the Raman and absorption spectra and the details of the crystal structure offer a cogent explanation for it. The build up of negative charge on the oxygen of the benzoyl carbonyl is facilitated by hydrogen bonds from the backbone amide groups of Gly 114 and Phe 64, and the dipole of an α-helix. The build up of positive charge at the 4-position of the benzoyl ring is facilitated by hydrogen bonding between the side chain of Asp 145 and the hydroxy group. Moreover, the strength of the electric field acting on the bound ligand is markedly enhanced because the benzoyl ring is surrounded by a sheath of hydrophobic residues, with the opposing charges occurring at either end of the sheath.

The observed red-shift in the case of the N155G selenol-subtilisin mutant is 6 nm and is 11 nm for P225A thiol-subtilisin. Lockhart and Kim *(12)* have shown experimentally that the dipolar field of model helical peptides can induce red-shifts of 4−5 nm in the λ_{max} of covalently attached ligands such as *p*-amino benzoic acid. The red-shifts we observe for the acyl enzymes depend on both local dielectric constant and the difference in the ground and excited-state dipoles. Since neither of these is known, a direct comparison with Lockhart and Kim's results is not possible. However, the latter do provide some indication of the expected contribution of the α-helix dipole to the red shifts we see in the present work and, thus, are consistent with the model generated for the acyl N155G selenol-subtilisin.

The modeling experiments have been able to provide a rationale for the conformational populations determined by the Raman results. Moreover, they provide a molecular explanation for the onset of polarization in the second conformer found in the expanded active sites. This not withstanding, it should be remembered that the modeling has been undertaken at rather a crude level. One such crude approximation has been to assign fixed partial charges, and thus, for example, the molecular mechanics calculations fail to take into account the interaction between the glutamate 156 charged side chain and the induced partially positive charge on the nearby thiophene ring. Nevertheless, it is expected that the calculated interaction based on fixed partial charges in the present model represents a lower bound for the true strength of electrostatic interaction and therefore has some validity. The ideal calculation would be an ab initio quantum mechanical conformational search involving the entire active site and the bound ligand, requiring extensive computational resources. With the continuing developments in computational hardware and software, such calculations

might soon be feasible. However, the spectroscopic results will continue to provide the solid benchmarks against which the calculations must be tested.

CONCLUSIONS

Electrostatic effects are known to play an important role in enzyme catalysis. Here we have shown that by undergoing a simple conformational change in an active site, a substrate can go from a region of null electric field to one where it experiences strong electric polarization. Plausible active-site groups giving rise to these electric field effects in variants of subtilisin have been identified. This study is a good illustration of the highly vectorial nature of electric fields in the active site of enzymes. Though the current example is that for a nonphysiological substrate, such effects are likely to be important in enzyme−substrate complexes in physiological systems too.

The present work refines and extends our ideas on the causes of strong π electron polarization within a chromophore. In the three classes that have been examined in detail, the cysteine proteases, dehalogenase and the modified subtilisins, polarization is observed for an acyl chromophore when the latter is attached via a thioester bond at or near the N-terminus of an α-helix. The electron pulling effect of the α-helix dipole is combined with the electron pull exerted by hydrogen bonds to the acyl carbonyl. Evidence from the present studies and the crystal structure of dehalogenase suggests that strong polarization requires, in addition, a negatively charged group to be placed near the chromophore at the end opposite to the acyl carbonyl.

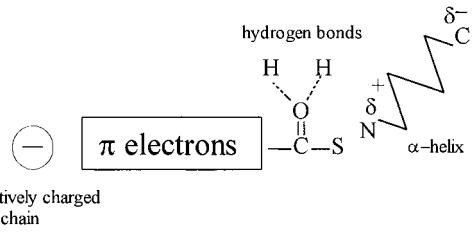

ACKNOWLEDGMENT

The authors are grateful to Dr. Megan O′Connor for the gift of 5-methyl-thienylacryloyl ethyl selenolester, to Dr. Eric Peterson for N155G selenol-subtilisin, and to Dr. James Wells for P225A thiol-subtilisin. Computational facilities at the Ohio supercomputer center are gratefully acknowledged.

REFERENCES

1. Cannon, W. R., Singleton, S. F., and Benkovic, S. J. (1996) *Nat. Struct. Biol. 3*, 821−33.
2. Warshel, A., and Sussman, F. (1986) *Proc. Natl. Acad. Sci. U.S.A. 83*, 3806−10.
3. Warshel, A., and Aqvist, J. (1991) *Annu. Rev. Biophys. Biophys. Chem. 20*, 267−98.
4. Desideri, A., Polticelli, F., Falconi, M., Sette, M., Ciriolo, M. R., Paci, M., and Rotilio, G. (1993) *Arch. Biochem. Biophys. 301*, 244−50.
5. Carey, P. R., and Tonge, P. J. (1995) *Acc. Chem. Res. 28*, 8−13.
6. Clarkson, J., Tonge, P. J., Taylor, K. L., Dunaway-Mariano, D., and Carey, P. R. (1997) *Biochemistry 36*, 10192−9.
7. Benning, M. M., Taylor, K. L., Liu, R. Q., Yang, G., Xiang, H., Wesenberg, G., Dunaway-Mariano, D., and Holden, H. M. (1996) *Biochemistry 35*, 8103−9.
8. Carey, P. R., Carriere, R. G., Lynn, K. R., and Schneider, H. (1976) *Biochemistry 15*, 2387−93.
9. Kim, M., Owen, H., and Carey, P. R. (1993) *Appl. Spectrosc. 47*, 1780−3.
10. Dong, J., Dinakarpandian, D., and Carey, P. R. (1998) *Appl. Spectrosc. 52*, 1117−22.
11. Doran, J. D., and Carey, P. R. (1996) *Biochemistry 35*, 12495−502.
12. Lockhart, D. J., and Kim, P. S. (1992) *Science 257*, 947−51.
13. Lockhart, D. J., and Kim, P. S. (1993) *Science 260*, 198−202.
14. Sitkoff, D., Lockhart, D. J., Sharp, K. A., and Honig, B. (1994) *Biophys. J. 67*, 2251−60.
15. Kortemme, T., and Creighton, T. E. (1995) *J. Mol. Biol. 253*, 799−812.
16. Sancho, J., Serrano, L., and Fersht, A. R. (1992) *Biochemistry 31*, 2253−8.
17. Katti, S. K., LeMaster, D. M., and Eklund, H. (1990) *J. Mol. Biol. 212*, 167−84.
18. Sheridan, R. P., and Allen, L. C. (1980) *Biophys. Chem. 11*, 133−6.
19. Aqvist, J., Luecke, H., Quiocho, F. A., and Warshel, A. (1991) *Proc. Natl. Acad. Sci. U S A 88*, 2026−30.
20. Markland, F. S., and Smith, E. L. (1970) *Enzymes 3*, 561−608.
21. Philipp, M., and Bender, M. L. (1983) *Mol. Cell. Biochem. 51*, 5−32.
22. Wu, Z.-P., and Hilvert, D. (1989) *J. Am. Chem. Soc. 111*, 4513−4.
23. Nakatsuka, T., Sasaki, T., Kaiser, E. T. (1987) *J. Am. Chem. Soc. 109*, 3808−10.
24. Abrahmsen, L., Tom, J., Burnier, J., Butcher, K. A., Kossiakoff, A., and Wells, J. A. (1991) *Biochemistry 30*, 4151−9.
25. Tonge, P. J., Pusztai, M., White, A. J., Wharton, C. W., and Carey, P. R. (1991) *Biochemistry 30*, 4790−5.
26. O'Connor, M. J., Dunlap, R. B., Odom, J. D., Hilvert, D., Pusztai-Carey, M., Shenoy, B., C., and Carey, P. R. (1996) *J. Am. Chem. Soc. 118*, 239−40.
27. Tonge, P., and Carey, P. R. (1989) *J. Mol. Liq. 42*, 195−212.
28. Peterson, E. B., and Hilvert, D. (1997) *Tetrahedron 53*, 12311−7.
29. Frisch, M. J., Trucks, G. W., Schlegel, H. B., Gill, P. M. W., Johnson, B. G., Robb, M. A., Cheeseman, J. R., Keith, T., Petersson, G. A., Montgomery, J. A., Raghavachari, K., M. A. Al-Laham, Z., V. G., Ortiz, J. V., Foresman, J. B., Cioslowski, J., Stefanov, B. B., Nanayakkara, A., Challacombe, M., Peng, C. Y., Ayala, P. Y., Chen, W., Wong, M. W., Andres, J. L., Replogle, E. S., Gomperts, R., Martin, R. L., Fox, D. J., Binkley, J. S., Defrees, D. J., Baker, J., Stewart, J. P., and M. Head-Gordon, G., C., and Pople, J. A. (1995) Gaussian, Inc., Pittsburgh, PA.
30. Wiberg, K. B. (1965) *J. Am. Chem. Soc 87*, 1070.
31. Engler, E. M., Andose, J. D., and Schleyer, P. v. R. (1973) *J. Am. Chem. Soc. 95*, 8005.
32. Bott, R., Ultsch, M., Kossiakoff, A., Graycar, T., Katz, B., and Power, S. (1988) *J. Biol. Chem. 263*, 7895−906.
33. Brünger, A. T., Kuriyan J., and Karplus, M. (1987) *Science 235*, 458−46.
34. Fausto., R., Tonge, P. J., and Carey, P. R. (1994) *J. Chem. Soc., Faraday Trans.* 90, 3491−503.
35. Tonge, P. J., Carey, P. R., and Fausto, R. (1997) *J. Chem. Soc., Faraday Trans. 93*, 3619−24.
36. Dinakarpandian, D., Shenoy, B., Pusztai-Carey, M., Malcolm, B. A., and Carey, P. R. (1997) *Biochemistry 36*, 4943−8.
37. Bowles, A. J., George, W. O., and Maddams, D. B. (1969) *J. Chem. Soc. B*, 810.
38. Cottee, F. H., Straughan, B. P., Timmons, C. J., Forbes, W. F., and Shilton, R. (1967) *J. Chem. Soc. B*, 1146.
39. Braxton, S., and Wells, J. A. (1991) *J. Mol. Biol.* 266, 11797−800.
40. Wells, J. A., Powers, D. B., Bott, R. B., Graycar, T. P., and Estell, D. A. (1987) *Proc. Natl. Acad. Sci. U.S.A.* 84, 1219−23.

BI9902541